Send Orders for Reprints to reprints@benthamscience.ae

Current Drug Metabolism, 2017, *18*, 527-534

REVIEW ARTICLE

Helix-Coil Transition Signatures B-Raf V600E Mutation and Virtual Screening for Inhibitors Directed Against Mutant B-Raf

Srinivas Bandaru[1], Tharaparambil Gangadharan Sumithnath[2], Saphy Sharda[3,4], Sanskruti Lakhotia[3], Anudeep Sharma[3], Amrita Jain[3], Tajamul Hussain[5], Anuraj Nayarisseri[3,4,6] and Sanjeev Kumar Singh[6,*]

[1]Institute of Genetics and Hospital for Genetic Diseases, Osmania University, Hyderabad - 500 016, Telangana, India; [2]St. Martin's Engineering College, Jawaharlal Nehru Technological University, Hyderabad - 500 014, Telangana, India; [3]Bioinformatics Research Laboratory, Eminent Biosciences, Vijaynagar, Indore - 452 010, Madhya Pradesh, India; [4]In silico Research Laboratory, LeGene Biosciences Pvt Ltd, 91, Sector-A, Mahalakshmi Nagar, Indore - 452 010, Madhya Pradesh, India; [5]Center of Excellence in Biotechnology Research, College of Science, King Saud University, Riyadh - 11451, Saudi Arabia; [6]Computer Aided Drug Designing and Molecular Modeling Lab, Department of Bioinformatics, Alagappa University, Karaikudi-630 003, Tamil Nadu, India

ARTICLE HISTORY

Received: June 22, 2016
Revised: September 1, 2016
Accepted: September 5, 2016

DOI:
10.2174/1389200218666170503114611

Abstract: Mutation in the B-Raf at V600E has been well implicated in the carcinogenesis that makes it as an attractive therapeutic target. In the present study, we sought to identify the basis of V600E mutation at functional and structural grounds. The study also pursues to identify a candidate molecule with better pharmacological profiles than existing B-Raf inhibitors through computational approaches. The functional effects of V600E mutation was predicted using SIFT and Polyphen servers. Protein structural alterations were predicted using SDM server and RMSD calculations. In order to identify molecules with better pharmacological profile, virtual screening was performed considering existing B-Raf inhibitors *viz.*, Vemurafenib, Sorafenib, Dabrfenib, Trametinib which served as query molecules for Tanimoto based shape similarity search with a threshold of 95%. Aided by MolDock algorithm, high affinity similar compound against each query was retrieved. All the similar compounds were further tested for toxicity profiles and biological activity. In the present study, the SNP was shown to be highly vulnerable to malfunction and have damaging effects. Further mutated protein showed that the secondary structure was highly irregular and side chain hydrogen bonds were unsaturated. The superimposition of wild onto mutated V600E B-Raf revealed that there was a helix-coil transition occurring wherein residues Val 502, Leu 505, Arg506, Lys 507 assumed coiled conformation in the mutated B-Raf. Virtual screening investigation showed that SCHEMBL298689 akin to Vemurafenib has highest affinity than all the hitherto discovered compounds; in addition, SCHEMBL298689 had least toxicity and optimal bioactivity.

Keywords: B-Raf V600E, Mutational studies, Helix-Coil Transitions, Virtual Screening, ADMET profiling.

1. INTRODUCTION

B-Raf forms an important member of Raf family bestowed with protein kinase activity, which has been implicated in various clinical presentations of carcinomas [1]. B-Raf is known to play crucial role as an intermediary in the Ras-Raf signaling cascades which are responsible for normal cell growth, differentiation, survival and directing cell growth [2].

The oncogenic potential of B-Raf was established, wherein the mutated B-Raf was found as an independent factor to induce overactive downstream signaling MEK and ERK in approximately 7% of human cancer samples with a particularly high frequency of mutation in malignant melanomas [3].

Over 40 different missense B-Raf mutations have been found, but the vast majority of the B-Raf mutations (>90%) represent a single nucleotide change of T to A at nucleotide 1799 resulting in a valine → glutamate mutation at residue 600 (V600E) of the protein chain, resulting in constitutively active B-Raf [4]. B-Raf itself accounts for approximately 60% of melanomas, with greater than 90% of B-Raf mutations resulting from the substitution of glutamic acid for V600E and affecting the kinase domain of the protein [5]. The V600E point mutation allows B-Raf to signal independently of upstream cues, as a result of constitutively active oncogenic B-Raf, overactive downstream signaling *via* MEK and ERK leads to excessive cell proliferation and survival, resistance to apoptosis and growth independent of growth factors [6]. In addition, the oncological potential of B-Raf V600E mutation was ascertained from investigations conducted by Ouyang *et al.*, 2006 [7] which showed that, in cells cultured *in vitro*, (V600E) B-Raf is able to stimulate endogenous MEK [MAPK (mitogen-activated protein kinase)/ERK (extracellular-signal-regulated kinase) and ERK phosphorylation leading to an increase in cell proliferation, cell survival, transformation, tumorigenicity, invasion and vascular development [8]. At the clinical diagnosis, B-Raf V600E mutation was observed in approximately 50% of tumors which include some 50% melanoma tumors, 40% papillary thyroid tumors, 30% serous ovarian tumors [9], 10% colorectal and 10% prostate tumors [10].

Due to over activation of Ras-Raf signaling, oncogenic B-Raf has now surfaced as a potential oncological therapeutic target. Since, B-Raf is the main activator of other kinases like MEK, its inhibition forms a therapeutic rational, in blocking the cell proliferation and induction of apoptosis [11]. Potent inhibitors of V600E mutant B-Raf have revolutionized the treatment of metastatic mela-

*Address correspondence to this author at the Computer Aided Drug Designing and Molecular Modeling Lab, Department of Bioinformatics, Alagappa University, Karaikudi-630 003, Tamil Nadu, India;
Tel: +91 4565223342; E-mail: skysanjeev@gmail.com

1389-2002/17 $58.00+.00

noma as a result of high response rates and their rapid mode of action which have recently been proven to improve progression-free and overall survival. Since 2011, the specific B-Raf targeted agents, vemurafenib and dabrafenib, and the MEK inhibitor-trametinib, have been licensed for the treatment of patients with unrespectable or metastatic B-Raf mutant melanoma [12].

The therapeutic mechanism by which drugs like vemurafenib act is by the inhibition of downstream signaling by mutant B-Raf monomers. In addition, such drugs can also cause activation of downstream MEK by normal Raf homo- and heterodimers in non-B-Raf mutated cells [13], which has been shown to be caused by transactivation of the nondrug-bound partner in B-Raf to Craf heterodimers or Craf to Craf homodimers [14]. Earlier attempts to target Raf for therapeutic purposes have been unsuccessful. For example, the multi-targeted kinase inhibitor sorafenib was initially developed which was thought to inhibit Raf and its downstream signaling. Failure of sorafenib was later pinned down to its multi targeted approach wherein non-selective activation of Raf isoforms was observed [15, 16].

In the later years, better understanding of Raf isoforms led to the target specific drug discovery which led to the development of vemurafenib. The target specific drugs were developed with pyridoimidazolone group compatible with the ATP pocket-binding domain of B-Raf. Vemrafinib was selective and potent (>80%) and efficiently inhibited V600E protein [17, 18]. Such drugs had marked effects on apoptosis, proliferation, and blockade of downstream ERK phosphorylation. These findings translated into inhibition of growth in V600E mutant melanoma cell lines, as well as tumor regression in xenograft models [19].

As with other biological targeted agents, these drugs are associated with predictable patterns of adverse events. For instance, vemurafenib was shown to be highly potent for B-Raf V600E, nevertheless has been associated with activation of MEK/ERK in non-malignant tissue leading to mechanistic side effect resulting in lesions . The most common of all severity grades were rash (49%), arthralgia (39%), fatigue (34%), photosensitivity (31%), alopecia (26%) and nausea (19%). Forty-six percent of patients experienced AEs, which were most commonly cutaneous SCC (12%), rash (5%), liver function abnormalities (5%), arthralgia (3%) and fatigue (3%). In extreme cases dose reduction of inhibitors (dabrafenib) was needed in 28% of trial patients because of drug intolerance [20].

In the past several decades, there has been considerable improvement in treating cancer with chemotherapy, radiation, and surgery [21]. However, been successful, traditional methods of treating cancer often suffer with developing systemic side effects in patients , in addition develop of resistance, and sometimes sub-optimal drug concentrations reach the tumor site [22, 23]. Many recent advances in cancer therapy have centered on targeting oncogenes involved in proliferation and survival pathways specific to cancer cells [24-26]. Several targeted therapies for example vemurafenib has enjoyed great success for treating advanced melanoma [27]. However, in many cases, patients develop resistance when treated with single pathway targeted therapies because of the multigenic abnormalities in cancer cells which often allow them to evade the action of these agents. The ability of advanced melanoma to develop resistance to vemurafenib is a recent example of how tumors can bypass the point of inhibition, leading to disease recurrence and progression [28,29]. From the observation, it is now understood that single-target agents falls short in combating a multifactorial diseases such as cancer. Multi-Target Inhibitors (MTIs) are becoming more and more attractive in cancer therapy as they are often more effective and less prone to resistance development than monotherapies.

In the very recent years, nucleic acid-based nanoliposomes are being used because some pharmacological agents are not accessible to particular target oncogenic proteins. There are a large number of mutations and perturbations in cancer cells, however only a few play a role in disease progression. Vemurafenib has been successful in targeting specific inhibition of B-Raf V600E in melanoma cells [30], however, as mentioned afore, melanoma cells are highly heterogenous therefore compete tumour reversal often fails. Such studies prove that that only a targets are able to be inhibited with current technologies [31], therefore there is a need of advanced therapeutic strategy to inhibit various target pathways for utmost management of cancer [32]. As an future drug therapeutics , there is great promise for siRNA-based nanoliposomal drug delivery to targ*et al*l the pathways involved in cancer, since this technique can make almost any oncogene a potential therapeutic target.

In the view of above, in the present study we put forth structural rationales of B-Raf V600E mutation and considering the adverse events associated with the established inhibitors, the study centers to identify high affinity B-Raf inhibitor with optimal ADMET properties through computational approaches.

2. MATERIALS AND METHODS

2.1. Analysis of B-Raf V600E Mutation

2.1.1. Prediction of Damaging Effect of SNP (B-Raf V600E)

The vulnerability of SNP (rs113488022) A→T in the B-Raf gene was evaluated thorough different mutation effect prediction servers like SIFT, Ensemble's mutation effect predictor. SIFT involves the effect of SNP on distortion in the protein structure thereby leading to decline activity of the protein. Variant Effect Predictor (VEP) involves SIFT scoring prediction in addition involves Polyphen-Proven score prediction which is efficient in predicting the effect of SNP at the transcript level [33]

2.1.2. Structural Analysis of B-Raf V600E Mutation

The crystal structure of B-Raf V600→E was retrieved from Protein Data Bank (PDB) with PDB ID: 4MNF [34]. The structure was prepared and further amino acids substitutions at 600^{th} position in the B-Raf structure was generated by Molegro Virtual Docker software 2010.4.0.0. The structure obtained from mutation was further energy minimized and optimized. The change in the protein structure accounting to amino acid mutation was analyzed by employing an online server - Site Directed Mutator (SDM) [35, 36]. SDM - a statistical potential energy function helps in analyzing single nucleotide polymorphisms (SNPs) that affect the structure or function of proteins and predicts the probability of malfunctioning of receptors in terms of protein stability. In the further step, local superimpositions of wild and mutated B-Raf was carried out to predict the RMSD to measure the deviation of mutated protein with its wild counterparts.

2.1.3. Selection of Inhibitors and Structure Similarity Search

Eight potential FDA approved B-Raf V600E inhibitors - Vemurafenib, Sorafenib, Dabrafenib, Trametinib served as query molecules for shape similarity search.

2.1.4. Preparation of Protein and Compounds

The crystal structure of B-Raf V600→E was retrieved from Protein Data Bank (PDB) with PDB ID: 4MNF [34]. The protein was prepared using the PrepWiz module of Schrodinger suite. In the preparation procedure, the protein was first preprocessed by assigning the bond bonders and hydrogen, creating zero order bonds to metals and adding disulphide bonds. The missing side chains and loops were filled using Prime Module of Schrodinger. Further all the water molecules were deleted beyond 5 Å from hetero groups. Once the protein structure was preprocessed, H bonds were assigned which was followed by energy minimization by OPLS 2005 force field. The final structure obtained was saved in .pdb format for further studies. All the ligands were optimized through OPLS 2005 force field algorithm [37] embedded in the LigPrep module of Schrödinger suite, 2013 (Schrodinger. LLC,

New York, NY). The ionizations of the ligand were retained at the original state and were further desalted. The structures thus optimized were saved in .sdf format for docking procedures [38].

2.1.5. Structure Similarity Search

The compound with superior pharmacological profile amongst all the established inhibitors were further used as query molecule in pursuit to identify still better drug like compound than any established inhibitor. Similarity search was supervised by Binary Finger Print Based Tanimoto similarity equation to retrieve compounds with similarity threshold of 95 % against NCBI's Pubchem compound database.

2.1.6. Molecular Docking of Compounds

Molecular docking program- Molegro Virtual Docker (MVD) which incorporates highly efficient PLP (Piece wise Linear potential) and MolDock scoring function provided a flexible docking platform [39]. All the ligands were docked at the active site of the B-Raf structure (PDB: 4MNF) with reference to co-crystallized ligand- GDC0879 (2-{4-[(1E)-1-(hydroxyimino)-2,3-dihydro-1Hinden-5-yl]-3-(pyridin-4-yl)-1H-pyrazol-1-yl}ethanol)). Docking parameters were set to 0.20Å as grid resolution, maximum iteration of 1500 and maximum population size of 50. Energy minimization and hydrogen bonds were optimized after the docking. Simplex evolution was set at maximum steps of 300 with neighborhood distance factor of 1. Binding affinity and interactions of ligands with protein were evaluated on the basis of the internal ES (Internal electrostatic Interaction), internal hydrogen bond interactions and sp2-sp2 torsions. Post dock energy of the ligand-receptor complex was minimized using Nelder Mead Simplex Minimization (using non-grid force field and H bond directionality) [40]. On the basis of rerank score, best interacting compound was selected from each dataset.

2.1.7. Bioactivity and ADMET Profiling of Compounds

All the compounds were screened for its drug ability by lipinksi filters. Biological activity of the ligands was predicted using Molinspiration webserver (© MolinspirationCheminformatics 2014). The complete ADMET properties was calculated using admetSAR [41]

2.1.8. Pharmacophoric Mapping

Pharmacophoric mapping which involves ligand interaction patterns, hydrogen bond interaction, hydrophobic interactions was evaluated using Accelrys Discovery Studio 3.5 DS Visualizer [42].

2.1.9. Softwares, Suites and Webservers Used

All the chemical structures were drawn in MarvinSketch 5.6.0.2, (1998-2011, Copyright © ChemAxon Ltd). Ligands were optimized with LigPrep module of Schrodinger suite 2013. Protein was processed and refined with protein preparation wizard of Schrodinger suite 2013 (Schrodinger. LLC, 2009, New York, NY). Flexible molecular docking of the compounds with target was completed using Molegro Virtual Docker 2010.4.0.0. Accelrys Discovery Studio® Visualizer 3.5.0.12158 (Copyright© 2005-12, Accelrys Software Inc.) was used for molecular visualizations. T.E.S.T software (2012, U.S. Environmental Protection Agency) and Molinspiration web server (© MolinspirationCheminformatics 2014) were respectively used for predicting LC50 and bioactivity of the compound. ADMET profiles were calculated using admetSAR (Laboratory of Molecular Modeling and Design. Copyright @ 2012, East China University of Science and Technology, Shanghai Key Laboratory for New Drug Design).

3. RESULTS AND DISCUSSION

The V600E point mutation is implicated as constitutively active oncogenic B-Raf independent of upstream signals, as a result, excessive cell proliferation and survival, resistance to apoptosis is observed leading to cancers. In assertion to the given physiological damage of the SNP, the prediction results revealed by SIFT (Table **1**) and Polyphen (Table **2**) showed that the SNP is highly vulnerable to malfunction and have damaging effects. In the further approach we pursued to study the effect of V600E mutation on the B-Raf structure and result were quite appreciable. There was a massive decline in the solvent accessible surface area of mutated B-Raf, in addition, secondary structure was highly irregular and side chain hydrogen bonds were considerably unsaturated (Table **3**). In order to find the comparative change in the structures of the protein we superimposed mutate protein onto wild protein. The results thus obtained were quite interesting as there was a gross change in the protein structure upon mutation which is reflected by high RMS of 1.932 (Table **4**). In the further perusal we noticed that the V600E mutation though did not affect the exact region of mutation *i.e.* at the 600th position but it grossly affected the local conformation from residues 500-507 wherein helix to coil transition was observed. The mutation lead to loss of well-ordered helix conformation to coil in mutated B-Raf (Fig. **1**). These observations support the drastic change in the mutated B-Raf indicating its significant departure in

Table 1. Prediction of SNP vulnerability by SIFT program. The program predicts the SNP to be highly damaging.

SNP	Amino Acid Change	Protein ID	Amino Acid	Using Orthologues in the Protein Alignment		Using Homologues in the Protein Alignment	
				Prediction	Score	Prediction	Score
rs113488022	V600E	NP_004324	V	TOLERATED	1.00	TOLERATED	1.00*
			E	DAMAGING	0.00	DAMAGING	0.00*

(Least the score higher is the damaging potential of the SNP. Score range 0.0-1.0)

Table 2. Prediction of SNP vulnerability by VEP program. The SIFT along with the Polyphen Proven score prediction system in VEP shows the mutation to be a misense variant with high damaging potential.

Uploaded variation	Location	Allele	Consequence	Impact	Exon	Protein position	Amino acids	Codons	SIFT	PolyPhen
rs113488022	7:140753336-140753336	T	missense variant	MODERATE	15	600	V/E	GTG/GAG	Deleterious (0.00)*	damaging (0.967)**

(Least the score higher is the damaging potential of the SNP. Score range 0.0-1.0) (**higher the score greater is the damaging potential of the SNP. Score range 0.0-1.0)

Table 3. Prediction of stability and protein malfunctioning in mutated receptor (V600E) by SDM server. The statistical potential energy function of SDM predicts the mutation to be highly stable in addition disease cause malfunction.

Structure State	AMINO ACID	Position	Secondary Structure	Solvent Accessibility	Side Chain Hydrogen Bond Satisfaction	Pseudo ΔΔ G
WILD	V	600	loop	53.80%	NO_HBONDS	-0.72
MUTATED	E		irregular	0.39%	UNSATURATED	
Prediction:	The mutation is predicted to be highly stabilizing and cause protein malfunction or disease					

Table 4. RMSD calculation Wild (V600) against mutated (E600) B-Raf.

Structures	RMSD	Max Diff
Wild *vs* Mutated	1.9341	31.7674 (atoms of 4156 & 4156)

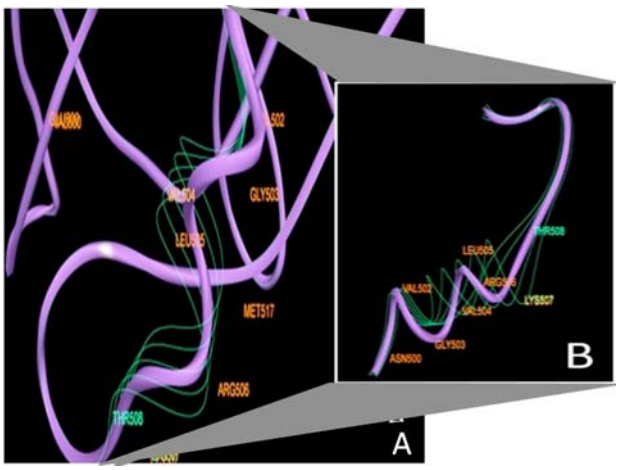

Fig. (1). (**a**)The mutated protein (solid purple coil) superimposed on wild protein structure (Green wire frame helix). The mutation leads to global perturbation leading to Helix-coil transitions at residues Val 502, Leu 505, Arg506, Lys 507. (**b**) magnified region of helix-coil transition.

the structural configurations from wild B-Raf. The structural aberration in the mutated receptor perhaps may explain its aberrant function by affecting its interaction to binding partners, and thereby signals for abnormal cell division leading to cancers.

In the further perusal, we sought to identify a small molecule bestowed with high affinity against mutate B-Raf than the established inhibitors. Number of similar compounds screened with ≥95 similarity corresponding to each parent compound and their best docked similar compounds against B-Raf is shown in Table **5** and (Fig. **2**). As evident from affinity (rerank) score, amongst all the parent inhibitors, vemurafenib showed highest and optimal affinity against B-Raf. However, it was SCHEMBL298689 CID: 87088960 a molecule akin to vemurafenib which showed highest affinity against B-Raf V600E. SCHEMBL298689 showed 1.02 folds higher affinity than vemurafenib further testifying it to be a high affinity molecule than any other compound in the present study.

The superior affinity of compound SCHEMBL298689 CID: 87088960 can be attributed to its excellent interaction profile especially in terms of electrostatic and H-bonding interactions. Apparent from the docking profile of compound energy values (Table **6**) of descriptors of external ligand interactions contributes higher stability than internal ligand interactions. Further external ligand interactions were stabilized mostly by steric energy guided by piece wise linear potentials. While in internal ligand interactions, the torsional strain contributes for the stability of the ligand receptor interactions. Owing to its high affinity than parent inhibitors and respective similar molecules we put forth SCHEMBL298689 as a high affinity potentiator of V600E B-Raf.

Further, we tested for activity against different drug targets (Table **7**), above all, it was SCHEMBL298689 which demonstrated

Table 5. Number of similar compounds retrieved through structure based similarity search against parent compounds. The affinity scores of parent and similar is listed.

Parent Compound	Rerank Score	Number of Similar Compounds Obtained with 95% Similarity	Best Docked Similar Compound (With Respect to Parent)	Rerank Score
Vemurafenib	-126.420	84	SCHEMBL298689 CID: 87088960	-128.326
Sorafenib	-113.487	153	SCHEMBL10105563 CID: 88567311	-116.252
Dabrafenib	-111.254	33	SCHEMBL12669795 (CID: 68345297)	-111.324
Trametinib	-102.555	19	SCHEMBL13163715 CID: 59717522	-100.555

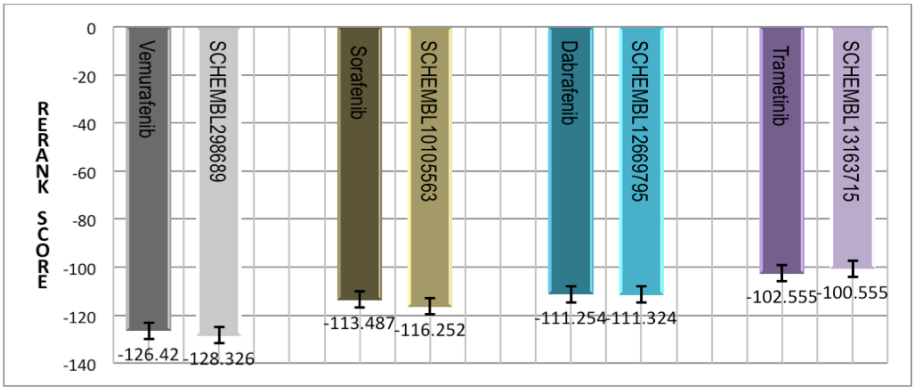

Fig. (2). Graph showing affinity (Rerank scores) of parent and respective similar. Vemurafenib similar SCHEMBL298689 shows highest affinity than all the studied compounds (including parent and respective similar).

Table 6. Energy Descriptor values for the affinity of Vemurafenib and its respective similar -SCHEMBL298689 against V600E B-Raf.

Energy Descriptors	VemuRafenib	SCHEMBL298689
	Rerank Score	Rerank Score
Total Energy	-128.33	-126.42
External Ligand interactions	-155.21	-154.52
Protein - Ligand interactions	-155.21	-154.52
Steric (by PLP)	-122.09	-139.32
Steric (by LJ12-6)	-28.393	-12.178
Hydrogen bonds	-4.73	-3.027
Hydrogen bonds (no directionality)	0	0
Electrostatic (short range)	0	0
Electrostatic (long range)	0	0
Internal Ligand interactions	26.887	28.101
Torsional strain	4.395	4.397
Torsional strain (sp2-sp2)	0	0
Hydrogen bonds	0	0
Steric (by PLP)	4.014	5.987
Steric (by LJ12-6)	18.478	17.717
Electrostatic	0	0

highest kinase activity and least activity against other drug targets (demonstrating it to be target specific), which in addition testifies it to be the better potentiator of B-Raf.

Owing to better interaction profiles and activity, the toxicity testing still mandates a compound to be a bonafide drug. Therefore in the view we tested the carcinogenic as well as mutation profiles of the screened compound (Table **8**). Out of screened compounds SCHEMBL12669795(CID: 68345297) a compound akin to Dabrafenib was shown to be Ames toxic while others proved to be non-toxic and demonstrate safety profiles. Further, it can be noted that, along with good affinity profile and appreciable kinase activity, SCHEMBL12669795was neither carcinogenic nor mutagenic therefore qualifying to be a better inhibitors amongst the screened compounds in the study. Table **6** shows the complete ADMET profile of all the best docked similar compounds.

Owing to appreciable affinity profile, high kinase activity and non-toxic characteristic of SCHEMBL12669795, it was further mapped for its pharmacophoric properties. As shown in Fig. (**3A**), in the inhibitory cavity of B-Raf, the compound is hydrogen bond donor to Cys 532. There were van der waals contacts with Ala 481, Ile 463, Trp 531, Phe 583, Ile 527, Phe 516, Leu 505, Gly 466 and electrostatic contacts with Leu 514, Cys 532, Thr 529, Lys 483, Glu 501, Ser 536 and Phe 595. Further, the interactions are further strengthened by pi-pi interactions between the compound and residues like Lys 483. The electrostatic and hydrophobic interactions of the compound in the active site is shown in Fig. (**4a** and **b**) respectively.

Table 7. Bioactivity prediction of best docked similar compounds against various drug targets.

Compound	GPCR Ligand	Ion Channel Modulator	Kinase Inhibitor	Nuclear Receptor Ligand	Protease Inhibitor	Enzyme Inhibitor
SCHEMBL298689 CID: 87088960	0.15	-0.12	1.25	-0.11	-0.17	0.22*
SCHEMBL10105563 CID: 88567311	-0.07	-0.30	-0.20	-0.30	-0.08	0.18
SCHEMBL12669795 (CID: 68345297)	0.11	0.06	-0.24	-0.18	-0.05	-0.03
SCHEMBL13163715 CID: 59717522	-0.11	-0.51	-0.35	-0.43	-0.13	-0.08

Compound SCHEMBL298689 CID: 87088960showing highest kinase activity and least bioactivity against other drug targets testifying its target specificity against kinases(in the present case B-Raf V600E)

Table 8. ADMET profiles of best docked similars.

	SCHEMBL298689 (CID: 87088960)		SCHEMBL10105563 (CID: 88567311)		SCHEMBL12669795 (CID: 68345297)		SCHEMBL13163715 (CID: 59717522)	
Model	**Result**	**Probability**	**Result**	**Probability**	**Result**	**Probability**	**Result**	**Probability**
Absorption								
Blood-Brain Barrier	BBB+	0.746	BBB-	0.605	BBB+	0.909	BBB+	0.842
Human Intestinal Absorption	HIA+	0.993	HIA+	0.855	HIA+	0.991	HIA+	0.834
Caco-2 Permeability	Caco2-	0.561	Caco2-	0.651	Caco2-	0.575	Caco2-	0.537
P-glycoprotein Substrate	Substrate	0.837	Substrate	0.679	Substrate	0.792	Substrate	0.809
P-glycoprotein Inhibitor	Inhibitor	0.891	Non-inhibitor	0.647	Inhibitor	0.753	Inhibitor	0.782
Distribution & Metabolism								
CYP450 2C9 Substrate	Non-substrate	0.807	Non-substrate	0.828	Non-substrate	0.799	Non-substrate	0.836
CYP450 3A4 Substrate	Substrate	0.798	Substrate	0.555	Substrate	0.695	Substrate	0.657
CYP450 1A2 Inhibitor	Non-inhibitor	0.654	Inhibitor	0.572	Non-inhibitor	0.555	Non-inhibitor	0.771
CYP450 2D6 Inhibitor	Non-inhibitor	0.810	Non-inhibitor	0.785	Non-inhibitor	0.809	Non-inhibitor	0.578
CYP450 3A4 Inhibitor	Inhibitor	0.667	Inhibitor	0.763	Inhibitor	0.811	Inhibitor	0.705
Excretion & Toxicity								
Human Ether-a-go-go-Related Gene Inhibition	Inhibitor	0.6113	Inhibitor	0.6655	Inhibitor	0.7666	Inhibitor	0.8209
AMES Toxicity	Non-AMES toxic	0.532	Non AMES toxic	0.572	AMES toxic*	0.964	Non AMES toxic	0.700
Carcinogens	Non-carcinogens	0.686	Non-carcinogens	0.930	Non-carcinogens	0.762	Non-carcinogens	0.945
Honey Bee Toxicity	Low HBT	0.664	Low HBT	0.805	Low HBT	0.599	Low HBT	0.837
Acute Oral Toxicity	III	0.596	III	0.675	III	0.5766	III	0.708

* Compound SCHEMBL12669795similar to DaB-Rafenib demonstrating AMES toxicity, with high probability value therefore can be excluded from further pharmacological investigation.

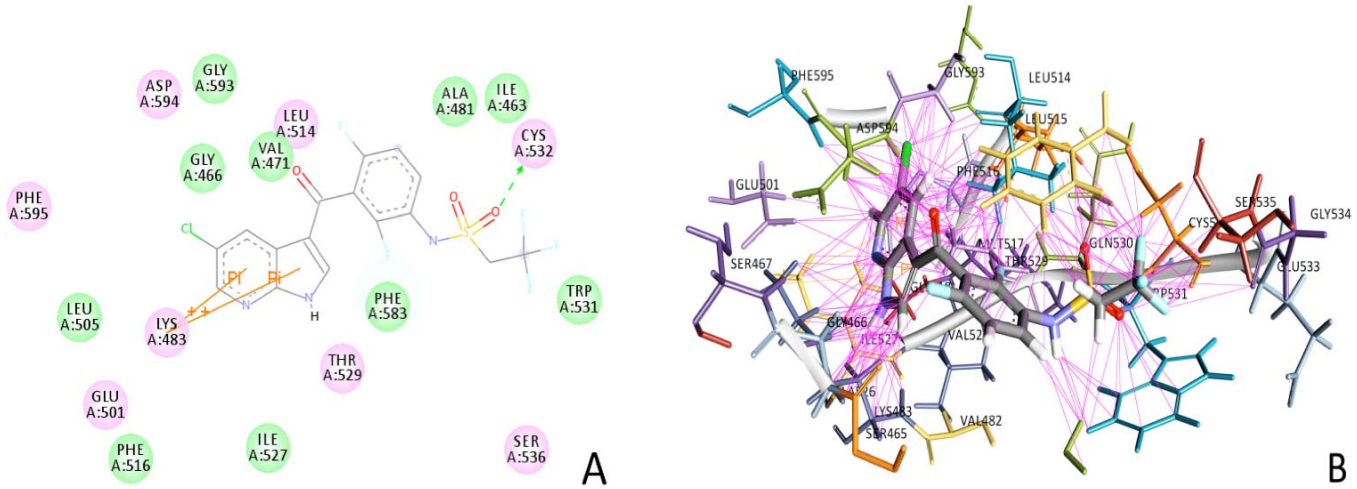

Fig. (3). A) Interactions of SCHEMBL298689 in the cavity of B-Raf V600E protein. Residues circled in green participate in van der Waals interaction with the ligand while residues in pink forms electrostatic interactions. Hydrogen bonds are shown as green arrows between ligand and residues Arg 498 and 501; **B**) Binding pattern of SCHEMBL298689 in the cavity. The pink lines represent various interactions like electrostatic, van der Waals, stearic, hydrogen bonding and hydrophobic interactions that enable energetically favorable binding of the ligand in the cavity.

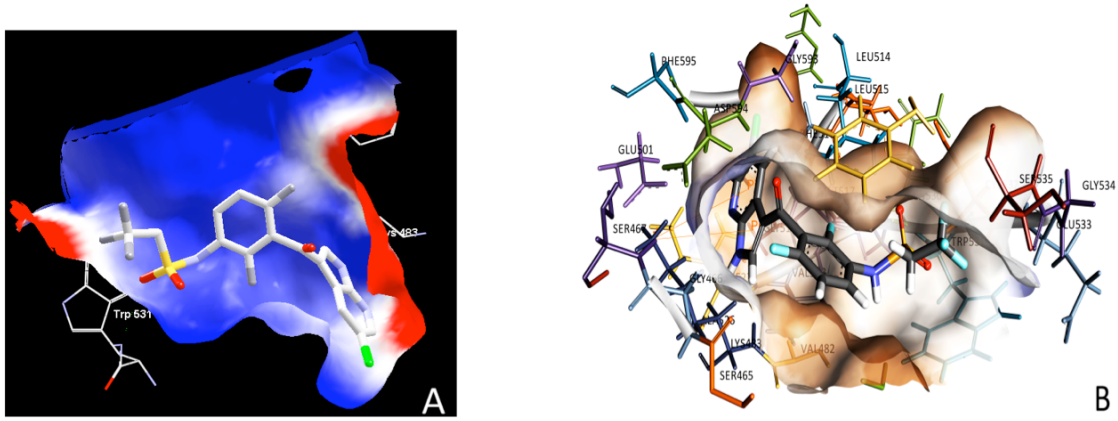

Fig. (4). A) SCHEMBL298689 deeply embedded in the cavity surrounded by highly electropositive residues; **B**) The channel harboring SCHEMBL298689 is shown with hydrophobic intensities. The hydrophobic intensities of the binding site ranges from least hydrophobic area - blue shade to highly hydrophobic area –brown shade).

Owing to high affinity against B-Raf V600E, appreciable interaction profiles and better ADMET and bioactivity we anticipate SCHEMBL298689 can overcome the narrow therapeutic window of present B-Raf inhibitors and can be to put forth for pharmacodynamics and pharmacokinetic experiments for better clinical outcomes in the successful treatment of cancers.

CONCLUSIONS

The BRaf mutation being an aisle for causing cancer. In the present study, we radicalized the impact of V600E mutation at the structural and functional planes, wherein the mutation leads to drastic Helix-coil transition in secondary structure. The study also endeavors to identify SCHEMBL298689 as a potential V600E B-Raf inhibitor endowed with enhanced therapeutic properties, appreciable kinase activity, least toxicity and least bioactivity than hitherto administered Vemurafenib.

CONSENT FOR PUBLICATION

Not applicable.

CONFLICT OF INTEREST

The authors confirm that this article content has no conflict of interest.

ACKNOWLEDGEMENTS

Funding from Council of Scientific and Industrial Research (CSIR), India, is highly acknowledged (Grant Number: 09/132 (0827)/2014-EMR-I).

REFERENCES

[1] Chong, H.; Vikis, H.G.; Guan, K.L. Mechanisms of regulating the Raf kinase family. *Cell. Signal.*, **2003**, 15*(5)*, 463-469.

[2] Davies, H.; Bignell, G.R.; Cox, C.; Stephens, P.; Edkins, S.; Clegg, S.; Davis, N. Mutations of the B-Raf gene in human cancer. *Nature*, **2002**, 417*(6892)*, 949-954.

[3] Tanzosh, E.E. Signaling networks that induce melanomagenesis and metastasis that can be exploited for therapeutic benefit., **2013.**

[4] Lupi, C.; Giannini, R.; Ugolini, C.; Proietti, A.; Berti, P.; Minuto, M.; Basolo, F. Association of B-Raf V600E mutation with poor clinicopathological outcomes in 500 consecutive cases of papillary thyroid carcinoma. *J. Clin. Endocrinol. Metab.*, **2007** 92*(11)*, 4085-4090.

[5] Gollob, J.A.; Wilhelm, S.; Carter, C.; & Kelley, S.L. Role of Raf kinase in cancer: therapeutic potential of targeting the Raf/MEK/ERK signal transduction pathway. In *Semin. Oncol.* **2006**, 33*(4)*, 392-406. WB Saunders.

[6] Hatzivassiliou, G.; Song, K.; Yen, I.; Brandhuber, B.J.; Anderson, D.J.; Alvarado, R.; Morales, T. RAF inhibitors prime wild-type

RAF to activate the MAPK pathway and enhance growth. *Nature*, **2010**, 464*(7287)*, 431-435.

[7] Ouyang, B.; Knauf, J.A.; Smith, E.P.; Zhang, L.; Ramsey, T.; Yusuff, N.; Fagin, J.A. Inhibitors of RAF kinase activity block growth of thyroid cancer cells with RET/PTC or B-Raf mutations *in vitro* and *in vivo*. Clin Cancer Res., **2006**, 12*(6)*, 1785-1793.

[8] Gollob, J.A.; Wilhelm, S.; Carter, C.; Kelley, S.L. (2006, August). Role of Raf kinase in cancer: therapeutic potential of targeting the Raf/MEK/ERK signal transduction pathway. In *Seminars in oncology* (Vol. 33, No. 4, pp. 392-406). WB Saunders.

[9] Pritchard, C.; Carragher, L.; Aldridge, V.; Giblett, S.; Jin, H.; Foster, C.; Kamata, T. Mouse models for B-Raf-induced cancers. *Biochem. Soc. Trans.*, **2007**, 35*(5)*, 1329-1333.

[10] Cho, N.Y.; Choi, M.; Kim, B.H.; Cho, Y.M.; Moon, K.C.; Kang, G.H. (). B-Raf and KRAS mutations in prostatic adenocarcinoma. *Int. J. Cancer*, **2006**, 119*(8)*, 1858-1862.

[11] Wong, K.K. Recent developments in anti-cancer agents targeting the Ras/Raf/MEK/ERK pathway. *Recent Pat. on Anti-Cancer Drug Discov.*, **2009**, 4*(1)*, 28-35.

[12] Robert, C.; Karaszewska, B.; Schachter, J.; Rutkowski, P.; Mackiewicz, A.; Stroiakovski; Chiarion-Sileni, V. Improved overall survival in melanoma with combined daB-Rafenib and trametinib. *N. Engl. J. Med*., **2015**, 372*(1)*, 30-39.

[13] Joseph, E.W.; Pratilas, C.A.; Poulikakos, P.I.; Tadi, M.; Wang, W.; Taylor, B.S. The RAF inhibitor PLX4032 inhibits ERK signaling and tumor cell proliferation in a V600E B-Raf-selective manner. *PNAS*, **2010**, 107, 14903-8

[14] Poulikakos, P.I.; Zhang, C.; Bollag, G.; Shokat, K.M.; Rosen, N. RAF inhibitors transactivate RAF dimers and ERK signalling in cells with wild-type B-Raf. *Nature*, **2010**, 464, 427-30.

[15] Matallanas, D.; Crespo, P. New druggable targets in the Ras pathway? *Curr. Opin. Mol. Ther*., **2010**, 12, 674-83.

[16] Van Cutsem, E.; van de Velde, H.; Karasek, P.; Oettle, H.; Vervenne, W.L.; Szawlowski, A. Phase III trial of gemcitabine plus tipifarnib compared with gemcitabine plus placebo in advanced pancreatic cancer. *J. Clin. Oncol.*, **2004**, 22, 1430-8.

[17] Davies, H.; Bignell, G.R.; Cox, C.; Stephens, P.; Edkins, S.; Clegg, S. Mutations of the B-Raf gene in human cancer. *Nature*, **2002**, 417, 949-54.

[18] Curtin, J.A.; Fridlyand, J.; Kageshita, T.; Patel, H.N.; Busam, K.J.; Kutzner, H. Distinct sets of genetic alterations in melanoma. N. Engl. J. Med. **2005**, 353, 2135-47.

[19] Bollag, G.; Hirth, P.; Tsai, J.; Zhang, J.; Ibrahim, P.N.; Cho, H. Clinical efficacy of a RAF inhibitor needs broad target blockade in B-Raf mutant melanoma. *Nature*, **2010**, 467, 596-9.

[20] Hauschild, A.; Grob, J.J.; Demidov, L.V.; Jouary, T.; Gutzmer, R.; Millward, M.; Martín-Algarra, S. DaB-Rafenib in B-Raf-mutated metastatic melanoma: a multicentre, open-label, phase 3 randomised controlled trial. *The Lancet*, **2012**, 380*(9839)*, 358-365.

[21] Smalley, K.S.; Herlyn, M.; Towards the targeted therapy of melanoma. *Mini. Rev. Med. Chem*., **2006**, 6, 387-393.

[22] Duncan, R. The dawning era of polymer therapeutics. *Nat. Rev. Drug Discov*., **2003**, 2, 347-360.

[23] Langer, R. Drug delivery and targeting. *Nature*, **1998**, 392, 5-10.

[24] Das Thakur, M.; Salangsang, F.; Landman, A.S.; Sellers, W.R.; Pryer, N.K. Modelling vemurafenib resistance in melanoma reveals a strategy to forestall drug resistance. *Nature*, **2013**, 494, 251-255.

[25] Sharma, A.; Madhunapantula, S.V.; Gowda, R.; Berg, A.; Neves, R.I. Identification of aurora kinase B and Wee1-like protein kinase as downstream targets of (V600E) B-Raf in melanoma. *Am. J. Pathol*., **2013**, 182, 1151-1162

[26] Evans, M.S.; Madhunapantula, S.V.; Robertson, G.P.; Drabick, J.J. Current and future trials of targeted therapies in cutaneous melanoma. *Adv. Exp. Med. Biol.*, **2013**, 779, 223-255.

[27] Banaszynski, M.1.; Kolesar, J.M. VemuRafenib and ipilimumab: new agents for metastatic melanoma. *Am. J. Health Syst. Pharm.*, **2013**, 70, 1205-1210.

[28] Kudchadkar, R.; Paraiso, K.H.; Smalley, K.S. Targeting mutant B-Raf in melanoma: current status and future development of combination therapy strategies. *Cancer J.* **2012**, 18, 124-131

[29] Sullivan, R.J.; Flaherty, K.T. Resistance to B-Raf-targeted therapy in melanoma. *Eur. J. Cancer*., **2013**, 49, 1297-1304.

[30] Sharma, A.; Madhunapantula, S.V.; Gowda, R.; Berg, A.; Neves, R.I. Identification of aurora kinase B and Wee1-like protein kinase as downstream targets of (V600E) B-Raf in melanoma. *Am. J. Pathol*., **2013**, 182, 1151-1162.

[31] Dancey, J.E.; Bedard, P.L.; Onetto, N.; Hudson, T.J. The genetic basis for cancer treatment decisions. *Cell*., **2012**, 148, 409-420.

[32] Stegh, A.H. Toward personalized cancer nanomedicine - past, present, and future. *Integr. Biol. (Camb)*., **2013**, 5, 48-65.

[33] Ng, P. C.; Henikoff, S. SIFT: Predicting amino acid changes that affect protein function. *Nucleic acid. Res.*, **2003**, 31*(13)*, 3812-3814.

[34] Haling, J. R.; Sudhamsu, J.; Yen, I.; Sideris, S.; Sandoval, W.; Phung, W.; Morales, T. Structure of the B-Raf-MEK complex reveals a kinase activity independent role for B-Raf in MAPK signaling. *Cancer Cell*, **2014**, 26*(3)*, 402-413.

[35] Topham, C.M.; Srinivasan, N.; Blundell, T.L. Prediction of protein mutants based on structural environment-dependent amino acid substitution and propensity tables. *Protein Eng.*, **1997**, 10, 7-21.

[36] Bandaru, S.; Tiwari, G.; Akka, J.; Kumar Marri, V.; Alvala, M.; Ravi Gutlapalli, V.; Prasad, M.H.. Identification of high affinity bioactive salbutamol conformer directed against mutated (thr164ile) beta 2 adrenergic receptor. *Curr. Top. Medi. Chem.*, **2015**, 15*(1)*, 50-56.

[37] Jorgensen, W.L.; Maxwell, D.S.; Tirado-Rives, J. Development and testing of the OPLS all-atom force field on conformational energetics and properties of organic liquids. *J. Am. Chem. Soc*., **1996**, 118*(45)*, 11225-11236.

[38] Bandaru, S.; Ponnala, D.; Lakkaraju, C.; Bhukya, C.K.; Shaheen, U.; Nayarisseri, A. Identification of high affinity non-peptidic small molecule inhibitors of MDM2-p53 interactions through structure-based virtual screening strategies. *Asian Pac. J. Cancer Prev.*, **2014**, 16*(9)*, 3759-3765.

[39] Bandaru, S.M.; Hema, P.A.; Jyothy, A. N.; Mukesh, Y. Binding Modes and Pharmacophoric Features of Muscarinic Antagonism and β2 Agonism (MABA) Conjugates. *Curr. Top. Medi. Chem.*, **2013**, 13*(14)*, 1650-1655.

[40] Nelder, J. A.; Mead, R. A simplex method for function minimization. *Comput. J*., **1965**, 7*(4)*, 308-313.

[41] Cheng, F.; Li, W.; Zhou, Y.; Shen, J.; Wu, Z.; Liu, G.; Tang, Y. admetSAR: a comprehensive source and free tool for assessment of chemical ADMET properties. *J. Chem. Info. Mod*., **2012**, 52*(11)*, 3099-3105.

[42] Visualizer, D.S. Release 3.5. *Accelrys Inc., San Diego, CA, USA*. **2012**.